Author Manuscript

Author Manuscript

Author Manuscript

Author Manuscript

HHS Public Access

Author manuscript

Mol Pharm. Author manuscript; available in PMC 2023 December 05.

Published in final edited form as:

Mol Pharm. 2022 December 05; 19(12): 4612–4624. doi:10.1021/acs.molpharmaceut.2c00465.

Oral Nanocurcumin Alone or in Combination with Insulin Alleviates STZ-Induced Diabetic Neuropathy in Rats

Subhash Dwivedi[•],

College of Community Health Sciences, The University of Alabama, Tuscaloosa, Alabama 35487-0166, United States; The Center for Convergent Bioscience and Medicine (CCBM), and Alabama Life Research Institute, The University of Alabama, Tuscaloosa, Alabama 35487-0166, United States

Anuhya Gottipati,

College of Community Health Sciences, The University of Alabama, Tuscaloosa, Alabama 35487-0166, United States; The Center for Convergent Bioscience and Medicine (CCBM) and Alabama Life Research Institute, The University of Alabama, Tuscaloosa, Alabama 35487-0166, United States

Raghu Ganugula[•],

College of Community Health Sciences, The University of Alabama, Tuscaloosa, Alabama 35487-0166, United States; The Center for Convergent Bioscience and Medicine (CCBM), Alabama Life Research Institute, and Department of Biological Sciences, The University of Alabama, Tuscaloosa, Alabama 35487-0166, United States

Meenakshi Arora[•],

College of Community Health Sciences, The University of Alabama, Tuscaloosa, Alabama 35487-0166, United States; The Center for Convergent Bioscience and Medicine (CCBM), Alabama Life Research Institute, and Department of Biological Sciences, The University of Alabama, Tuscaloosa, Alabama 35487-0166, United States

Corresponding Author: **M. N. V. Ravi Kumar** – *College of Community Health Sciences, The University of Alabama, Tuscaloosa, Alabama 35487-0166, United States; The Center for Convergent Bioscience and Medicine (CCBM), Alabama Life Research Institute, and Department of Biological Sciences, The University of Alabama, Tuscaloosa, Alabama 35487-0166, United States; Chemical and Biological Engineering, University of Alabama, Tuscaloosa, Alabama 35487-0166, United States; Department of Pharmaceutical Sciences, Irma Lerma Rangel College of Pharmacy, Texas A&M University, College Station, Texas 77843, United States; Nephrology Research and Training Center, Division of Nephrology, Department of Medicine and Center for Free Radical Biology, University of Alabama at Birmingham, Birmingham, Alabama 35401, United States*; Phone: +1-205-348-2363; mnvrkumar@ua.edu.

[•]S.D., R.G., and M.A. contributed equally to this work.

Author Contributions

M.A. prepared the polymer and nCUR formulation, including its characterization. S.D., A.G., M.A., and R.G. involved in study execution, data acquisition and analysis. R.G. has performed the confocal imaging and analysis. M.N.V.R.K. conceptualized the project and data interpretation. S.D. and A.G. have written the draft. M.A., R.G., R.F., R.O., A.R.H., R.B., H.L.P., and M.N.V.R.K. edited the manuscript. All authors have approved the final version.

Supporting Information

The Supporting Information is available free of charge at https://pubs.acs.org/doi/10.1021/acs.molpharmaceut.2c00465.

Additional data sets complimenting the main body, viz., study design and characterization of representative nCUR preparations, and effect of treatment on animal body weights, hind paw morphology, peripheral nerves, Bielschowsky's silver and H&E staining of skin, sciatic nerve stained for NF200 (red), F4/80+ (green), and $CD3^+$ (turquoise), NLRP3 inflammasome in hind paw, Txnrd1 in sciatic nerve, terminal blood/plasma biochemistry, spleen weight and histology, autophagy markers in spinal cord and sciatic nerves of diabetic rats (PDF)

Complete contact information is available at: https://pubs.acs.org/10.1021/acs.molpharmaceut.2c00465

The authors declare no competing financial interest.

Author Manuscript Author Manuscript Author Manuscript Author Manuscript

Richard Friend,
College of Community Health Sciences, The University of Alabama, Tuscaloosa, Alabama 35487-0166, United States

Robert Osburne,
College of Community Health Sciences, The University of Alabama, Tuscaloosa, Alabama 35487-0166, United States

Aline Rodrigues-Hoffman,
Department of Comparative, Diagnostic & Population Medicine, College of Veterinary Medicine, University of Florida, Gainesville, Florida 32611-7011, United States

Rita Basu,
Division of Endocrinology, Center of Diabetes Technology, University of Virginia School of Medicine, Charlottesville, Virginia 22908, United States

Hui-Lin Pan,
Center for Neuroscience and Pain Research, Department of Anesthesiology and Perioperative Medicine, The University of Texas MD Anderson Cancer Center, Houston, Texas 77030, United States

M. N. V. Ravi Kumar
College of Community Health Sciences, The University of Alabama, Tuscaloosa, Alabama 35487-0166, United States; The Center for Convergent Bioscience and Medicine (CCBM), Alabama Life Research Institute, and Department of Biological Sciences, The University of Alabama, Tuscaloosa, Alabama 35487-0166, United States; Chemical and Biological Engineering, University of Alabama, Tuscaloosa, Alabama 35487-0166, United States; Department of Pharmaceutical Sciences, Irma Lerma Rangel College of Pharmacy, Texas A&M University, College Station, Texas 77843, United States; Nephrology Research and Training Center, Division of Nephrology, Department of Medicine and Center for Free Radical Biology, University of Alabama at Birmingham, Birmingham, Alabama 35401, United States; Phone: +1-205-348-2363

Abstract

Diabetes mellitus (DM), a multifaceted metabolic disorder if not managed properly leads to secondary complications. Diabetic peripheral neuropathy (DPN) is one such complication caused by nerve damage that cannot be reversed but can be delayed. Recently, diabetes patients are using dietary supplements, although there remains a general skepticism about this practice. Curcumin (CUR), one such supplement can help prevent underlying low-grade inflammation in diabetes, but it is plagued by poor oral bioavailability. To better understand the role of bioavailability in clinical outcomes, we have tested double-headed nanosystems containing curcumin (nCUR) on DPN. Because CUR does not influence glucose levels, we have also tested the effects of nCUR combined with long-acting subcutaneous insulin (INS). nCUR with or without INS alleviates DPN at two times lower dose than unformulated CUR, as indicated by qualitative and quantitative analysis of the hind paw, sciatic nerve, spleen, and L4–6 spinal cord. In addition, nCUR and nCUR+INS preserve hind paw nerve axons as evident by the Bielschowsky silver stain and intraepidermal nerve fibers (IENF) density measured by immunofluorescence. The mechanistic

Author Manuscript Author Manuscript Author Manuscript Author Manuscript

studies further corroborated the results, where nCUR or nCUR+INS showed a significant decrease in TUNEL positive cells, mRNA expression of NLRP3, IL-1β, and macrophage infiltration while preserving nestin and NF200 expression in the sciatic nerve. Together, the data confirms that CUR bioavailability is proportional to clinical outcomes and INS alone may not be one of the solutions for DM. This study highlights the potential of nCUR with or without INS in alleviating DPN and warrants further investigation.

Graphical Abstract

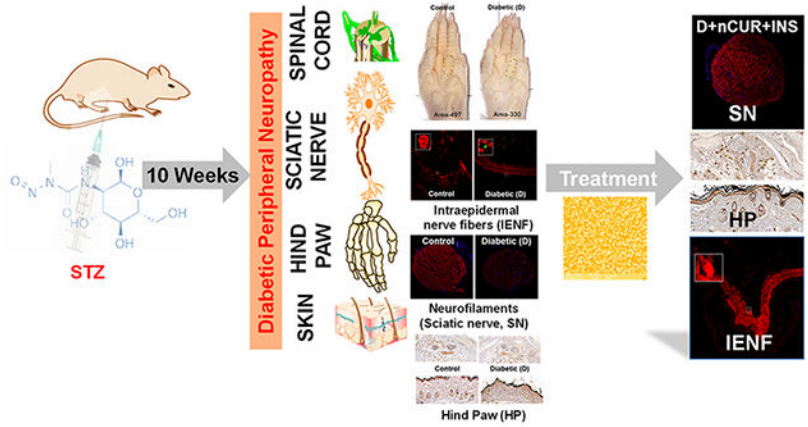

Keywords

bioavailability; combination therapy; curcumin; diabetic peripheral neuropathy; gambogic acid; nanoparticles; NLRP3 inflammasomes; oral delivery

INTRODUCTION

Diabetes is a metabolic disorder associated with hyperglycemic conditions due to impaired insulin secretion or impaired insulin action. As per the IDF Diabetes Atlas, approximately 537 million (in the age group 20–79 years) people globally are suffering from diabetes and have the propensity is to reach 783 million by the year 2045.[1] Almost 50% of the diabetic population is affected by diabetic peripheral neuropathy (DPN) and in certain patients it remains asymptomatic.[2] Distal symmetric neuropathy, accounts for 75% of diabetic neuropathies, affects large-fiber, small-fiber, or mixed fibers.[3] The primary symptoms of DPN include: numbness, a burning sensation, hyperesthesia, pain, and degeneration/loss of peripheral nerves, such as sciatic nerve and hind paw nerve fibers, which can result in foot ulcers and limb amputation.[4–6] A DPN diagnosis is routinely checked via diabetic foot screening for lower limb sensory and vascular deficits. When showing DPN symptoms, clinical scoring methods are available such as the Toronto Clinical Scoring Systems (TCSS) to assess the small and large nerve function. Both type 1 and type 2 diabetes are associated with a decreased intraepidermal nerve fiber-(IENF) density in humans. IENF density measurement by epidermal punch biopsy is a reliable clinical tool to assess the progression of DPN.[3,7]

Author Manuscript Author Manuscript Author Manuscript Author Manuscript

The underlying pathogenesis of DPN is complex, and hyperglycemia is considered a significant factor in the progression and development of DPN. Although rigorous control of glucose levels play a pivotal role in type 1 diabetes, similar control fails to reduce the progression of DPN in type 2 diabetes models,[8] which suggests the association of other pathways triggered by an initial higher or fluctuation in glucose levels. Increased glucose levels substantially activate the polyol and hexosamine pathways, resulting in increased reactive oxygen species (ROS) and inflammation.[4] Therapeutic and preventive management of DPN presents a significant challenge to the medical field due to the limited treatment options available. Serotonin-norepinephrine reuptake inhibitors (Duloxetine) and the $\alpha 2\delta$-1 inhibitory ligand (Pregabalin) are the only drugs approved by US Food and Drug Administration (USFDA) for treating painful DPN. However, these drugs are only effective in about 40% of the patients.[9]

Insulin (INS) plays a crucial role in glycemic control and neuroprotection. Therefore, loss of INS or insulin growth factor (IGF) support to the sensory neurons contributes to the development of IENF loss or shrinkage.[10] Although tight glucose control via INS is possible, it is associated with a risk of hypoglycemia. Therefore, a multifactorial interventional approach, besides glucose control, such as natural anti-inflammatory agents, is gaining wide acceptance as a preventive strategy. The development of efficient combined therapies such as INS with curcumin (CUR) may offer better protection against progressive DPN. CUR has effective antioxidant and anti-inflammatory properties and is well-tolerated at very high doses; however, its clinical translation is limited by poor solubility and permeability.[11] Several groups, including ours, use nanoparticle-based delivery systems which have improved the oral bioavailability of CUR.[12–16] Among all others, polyester-based systems appear to be a better delivery mechanism, owing to their ability to protect encapsulated compounds from harsh gastric conditions, customizable loading and release kinetics, and flexible chemistries for ligand conjugation for active transport across biological barriers.[17] CUR-laden PLGA nanoparticles improve CUR oral bioavailability by at least 9-fold compared to unformulated CUR[18] and delays progression of diabetic cataracts.[13] The PLGA-CUR nanoparticles are stable at room temperature and refrigerated storage conditions.[19] To further improve oral bioavailability of CUR, we used active delivery approaches.[12] In doing so, we have developed the next generation of PLGA nanoparticles, where the terminal functional group of PLGA is linked to a tripodal spacer that allows coupling of two ligand molecules [(gambogic acid-GA), GA_2], which traditionally was restricted to one ligand molecule. PLGA-GA_2-CUR (nCUR) leads to a 7-fold increase in oral bioavailability of CUR compared to conventional PLGA-CUR and 2-fold compared PLGA-GA-CUR nanoparticles, proving the hypothesis that double-headed are better than single-headed particles.[12] nCUR is safe and effective in alleviating intraocular inflammation in a canine model of lens-induced uveitis.[15]

In the present study, we report the efficacy of oral nCUR with and without subcutaneous INS in alleviating DPN in experimental diabetes induced by streptozotocin (STZ) in rats. This model mimics the clinical signs of DPN such as oxidative stress and inflammation.[14,20] The results of this pilot study can help to guide the design and implementation of larger scale efficacy studies that will further test the efficacy of nCUR+INS in DM and its complications.

Author Manuscript Author Manuscript Author Manuscript Author Manuscript

EXPERIMENTAL SECTION

Materials.

CUR was purchased from Acros Organics (USA). Streptozotocin (STZ) was procured from Sigma-Aldrich (USA). Unless noted, all other chemicals were purchased from Fisher Scientific (USA). Primers were obtained from Integrated DNA Technologies (IDT, USA), and qPCR reagents were obtained from Qiacube and BioRad. Long-acting INS (Lantus, Sanofi-Aventis, USA) was purchased through local vendors.

Synthesis of PLGA-GA_2.

The polymer synthesis was performed following prior developed protocols and involved simple 1-ethyl-3-(3-dimethyl aminopropyl) carbodiimide [EDC] cross-linking reaction with ligand and gambogic acid [GA] via the linker tris(2-aminoethyl) amine [TREN]. The synthesis protocols were thoroughly optimized and scaled. In brief, TREN-diBoc is connected to polylactide-*co*-glycolide (PLGA) 50:50, [Resomer 503H] via EDC, and subsequently deprotected, leaving two free amines, which were then conjugated with GA via EDC coupling. The GA conjugation was affirmed by using NMR, UV, and FTIR spectroscopy techniques. The presence of an N–H peak in the range of 8–9 ppm and GA peak at 6.3 in NMR spectra confirmed the formation of amide linkage between PLGA, linker, and GA. The amide bond formation was further confirmed by FTIR spectroscopy (1670–1630 cm^{-1} for C=O stretching, 1650–1560 cm^{-1} for N–H bending). The UV spectra further confirms the presence of GA characteristic peak at 365 nm before conjugation that is shifted to 390 nm for GA conjugated PLGA.[12,15]

PLGA-GA_2-CUR (nCUR) Nanoparticles.

A large-scale synthesis of nCUR was accomplished in 40 batches following prior developed oil-in-water single emulsion protocols.[12,15] In brief, the organic solution was prepared by dissolving PLGA-GA_2 (500 mg) and CUR (75 mg) in ethyl acetate (25 mL). This organic solution was added dropwise to water containing poly(vinyl alcohol) (50 mL) under continuous stirring. The oil-in-water emulsion was homogenized at 15000 rpm for 45 min and added to a solution of excess water (200 mL) to facilitate organic solvent evaporation overnight under stirring. The resulting nanoemulsion was centrifuged at 15000*g* for 30 min at 4 °C. The pellet was suspended in 25 mL of sucrose solution [5% (*w/v*)] and stored in a freezer at −80 °C. The nCUR was freeze-dried at −55 °C for 55 h under vacuum (0.002 mbar) using a benchtop freeze drier (Labconco Free Zone Triad), followed by heating cycles at 20 °C for 20 h under a vacuum (0.002 mbar). The freeze-dried samples were crimp-sealed and stored at 4 °C for future animal experiments. The dried nCUR upon resuspension was used to measure the size and morphology with dynamic light scattering (DLS, Malvern) and scanning electron microscopy (SEM, Tescan Vega 3 microscope) respectively. CUR entrapment was estimated using prior developed HPLC protocols.[12,15]

Author Manuscript Author Manuscript Author Manuscript Author Manuscript

Animal Study and Treatment.

Six-week-old male Sprague–Dawley rats (200 g, Envigo corporation, 46 rats) were used in this study. All the procedures were approved by the Texas A&M University Institutional Animal Care and Use Committee (IACUC 2020–0165).

To induce diabetes, rats were administered a single dose of streptozotocin (STZ) via intraperitoneal injection (55 mg/kg body weight), dissolved in 0.1 M citrate buffer (pH 4.5),[21] and naive rats, Group 1: Control (C) ($n = 6$). Blood glucose levels were monitored, followed by 72 h of STZ administration, including 16 h of fasting. Rats with blood glucose levels greater than 150 mg/dL were considered diabetic (D) and used for the study. Diabetic rats were placed into 5 groups. Group 2 (Diabetic-D) ($n = 8$); Group 3 (D+CUR) ($n = 8$): CUR suspended in CMC (0.5%) administered orally at 40 mg/kg/day; Group 4 (D+nCUR) ($n = 8$): nCUR orally at 20 mg CUR equivalent/kg/day suspended in deionized water; Group 5 (D+nCUR+INS) ($n = 8$): INS subcutaneously at 2 IU/rat daily and nCUR orally at 20 mg CUR equivalent/kg/day suspended in deionized water; and Group 6 (D+INS) ($n = 8$): only INS by subcutaneous route at 2 IU/rat daily for 10 weeks (study design presented in Figure S1A). During the study, animals had free access to normal pellet diet and water *ad libitum*.

Weekly general physically examination, including body weight recording, was performed by manual restraint procedures in order to avoid and/or limit pain and distress to the rat. Blood glucose was measured by the tail-prick method using a glucometer (Alphatrak blood glucose monitoring system Abbott Laboratories). After 10 weeks of treatment protocols, animals were sacrificed. Immediately after sacrificing, blood was collected from cardiac puncture and plasma was separated by centrifuging at 3000*g* for 30 min at 4 °C. Plasma biochemistry and hematology were performed at Texas A&M Veterinary Medical Diagnostic Laboratory (TVMDL). Hind paws, L4–6 spinal cord, sciatic nerve, and spleen were collected and stored at −80 °C or fixed in formalin for further analysis.

Histology.

Formalin-fixed right hind paw, sciatic nerve, and spleen samples were embedded in paraffin for histological evaluation. Hind paw sections were decalcified prior to tissue processing and sectioned at 5 μm thickness using a microtome. Slides were heated to 70 °C for 40 min in an oven, followed by deparaffinization in xylene, sequentially hydrated in 100, 95, and 70% ethanol, respectively, and subsequently washed in phosphate-buffered saline (PBS). Sections were incubated with antigen retrieval solution at pH 9 for 20 min and then washed twice in PBS. Sections were blocked with 3% goat serum for 20 min followed by triple washings in PBS.

Nerve fibers in sciatic nerve sections were stained with a nestin primary antibody (Cell Signaling Technology, Danvers, MA) at 1:100 dilution in 1.5% goat serum in PBS overnight at 4 °C followed by goat anti-mouse IgG Alexa Fluor-555 antibody at 1:1000 dilution for 2 h (Invitrogen, Waltham, MA). Intraepidermal nerve fibers (IENF) were stained in the hind paw using an IENF primary antibody (Millipore) at 1:100 dilution (1.5% goat serum in PBS) overnight at 4 °C followed by goat anti-rabbit IgG Alexa Fluor-594 at 1:1000 dilution (Invitrogen, Waltham, MA) for 2 h. To evaluate the cell death, the tissue sections were

Author Manuscript Author Manuscript Author Manuscript Author Manuscript

incubated with TUNEL reagent (*In Situ* Cell Death Detection Kit, POD Sigma-Aldrich) as per the manufacturer instructions, and TUNEL-positive cells were quantified in the peripheral nerve of the hind paw.

Sciatic nerve sections were triple-stained to visualize nerve fibers (NF200), T cells (CD3), and macrophages (F4/80). The sections were first incubated with a NF200 primary antibody (Sigma, St. Louis, MO) at 1:40 dilution in 1.5% goat serum overnight at 4 °C. Sections were triple-washed with PBS and incubated with goat anti-mouse IgG Alexa Fluor-555 antibody at 1:1000 dilution (Invitrogen, Waltham, MA) for 2 h. Sequential staining was performed on the same slides with a F4/80 primary antibody (Bio-Rad Hercules, CA) at 1:40 dilution in 1.5% goat serum overnight at 4 °C and incubated with 1:1000 dilution of goat anti-mouse IgG 488 secondary antibody (Invitrogen, Waltham, MA). Finally, sections were stained with 1:500 dilution of an APC/cyanine 7 CD3 antibody for 2 h at room temperature. After a final three times washing with PBS, mounting media with DAPI (Vectashield, Vector laboratories) was added, and cover-slipped. The stained slides were visualized under a confocal microscope (LSM 900, Zeiss), and eight representative images were taken from different rats within the same group and were used for quantification using ImageJ software (NIH).

Hematoxylin and eosin (H&E) staining was used on the right hind paw and spleen. Bielschowsky silver nitrate staining, a special staining for axons were performed at the College of Veterinary Medicine & Biomedical Sciences (CVBMS), Texas A&M University, core histology laboratories.

Real-Time PCR.

For qPCR studies, RNA was isolated from the spinal cord, sciatic nerve, and left hind paw using all prep DNA/RNA FFPE kit from Qiagen (Hilden, Germany). Samples were thawed, weighed and incubated in 150 μL of proteinase K digest (PKD) buffer and 10 μL of proteinase K (Qiagen) prior to homogenization on a hot plate at 56 °C for 3 min. Tissues were then homogenized using Precellys Lysing Kit, (Bertin instruments, France) in a bead blaster 24R (Benchmark) at 3600 rpm for 10 s, of three cycles at intervals of each 5 s. Homogenized samples were placed on the hot plate at 56 °C for 1 min prior to centrifuging at 13000 rpm at 4 °C for 2 min. Supernatant was collected into a 2 mL sample collection tube (Qiagen) and placed in the respective holders in QiACube (Qiagen), as per FFPE protocol. RNA was quantified using Take3 plate (Cytation 5, BioTek, Winooski, VT), and 60 ng/μL of RNA sample was used to prepare cDNA using a cDNA Synthesis Kit. cDNA was amplified using Sso Advanced Universal SYBR green Supermix in CFX Opus 384, RT-PCR (BioRad, Hercules, CA) for inflammatory, antioxidant, and autophagy markers (for primer sequences, refer Table 1). All the analyses were normalized against β-actin using ΔC_t values, where C_t is the threshold cycle. The fold change was expressed as $2^{-\Delta\Delta C_t}$ between the groups.

Statistical Analysis.

Statistical analysis of the quantitative data was carried out using one-way ANOVA and Tukey posthoc tests ($p < 0.05$ considered as significant) and student t test using GraphPad

Author Manuscript Author Manuscript Author Manuscript Author Manuscript

Prism 9.3.1. Data were presented as Mean ± standard error of mean (SEM). Unless otherwise stated, the diabetic group was compared with the control group, and the treated groups were compared with the diabetic group.

RESULTS

Characterization of nCUR.

The average size of the freeze-dried nCUR nanoparticles (40 batches) was ~270 nm (PDI ~ 0.25) (Figure S1B) and 0.112 mg of CUR is entrapped per mg of PLGA-GA_2. The representative SEM image of nCUR were presented in Figure S1C.

Health Monitoring.

Experimental animals were monitor for physical well being including body weights. Diabetic controls presented typical diabetes related symptoms (e.g., lethargic movement, loss of fur, sluggish response), while naïve animals did not. Diabetic rats showed progressive loss of body weight compared to naïve and nCUR+INS and INS treated groups, presented as percent change (Figure S2).

Effect of Treatment on Hind Paw Pad Morphology.

There was a significant decrease in the hind paw pad area of the diabetic group compared to the naïve rats that was matched by nCUR, nCUR+INS, and INS groups but not CUR (Figure 1A,B). These data were further supported by hind paw print analysis, where the inked area of diabetes rats was significantly reduced, while all treatment groups are similar to naïve rats (Figure S3). The paw length remained same across all groups (Figure 1C).

Effect of Treatment on Nerve Density in Hind Paw.

Bielschowsky staining was performed to quantify the axonal neurites in epidermal footpad tissues of the hind paw sections. As depicted in Figure 2A,B, a significant reduction in the stained brown areas indicates loss of axonal neurites in the diabetic group. Treatment with D+nCUR and D+nCUR+INS preserved axonal neurites, which were comparable to non-diabetic controls. On the other hand, CUR or INS alone groups failed to offer protection (Figure 2A,B). The same trends were evident by decreased IENF (Figure 3A,B) and increased TUNEL-positive cells in the diabetic group. All of the treatment groups preserved IENF fiber density, apart from CUR or INS groups that failed to prevent cell death (Figure 3A,C). Similarly, diabetes caused a reduction in small nerve fiber NF200 (Figure 4A,B) and an increase of macrophages ($F4/80^+$, Figure 4C) and T cells ($CD3^+$, Figure 4D). These changes were preserved largely by nCUR and nCUR+INS, but not CUR or INS alone (except for $CD3^+$). This data was further supported by an increase in peripheral nerve fibers identified by Bielschowsky staining, only in nCUR and nCUR+INS treatment groups (Figure 4E, F, Figure S4A). Representative images of H& E-stained peripheral nerves localization in right hind paw shown in Figure S4B. To understand the functional properties of the skin, we have performed Bielschowsky's silver and H&E staining of skin, showing changes in number and size of the sebaceous glands in diabetes groups that the treatment groups, nCUR and nCUR+INS offered some protection (Figure S5A,B), and this needs further investigation at biochemical and molecular levels.

Author Manuscript Author Manuscript Author Manuscript Author Manuscript

Effect of Treatment on Nerve Fiber and Inflammatory Status in Sciatic Nerve.

Sciatic nerve sections were stained with nestin to identify neuronal processes (Figure 5A). The quantitative data analysis showed reduced nestin staining in the diabetic group. All the treatment groups offered protection, however, and nCUR and nCUR+INS were more prominent in preserving neuronal intermediate filaments (Figure 5B).

Sciatic nerve sections were tripled stained (Figure 6A,Figure S6) with NF200 expression (staining neurofilament, red) and F4/80-positive (macrophages, green) and CD3-positive (T cells, turquoise) cells. Reduced NF200 expression (Figures 6B and S6) and increased F4/80 positive (Figure 6C) and CD3-positive cell (Figures 6D and S6) expression was observed in the diabetic group. All the treatment groups protected diabetes-induced changes at varied levels with nCUR and nCUR+INS most prominent except that CUR and INS failed to offer any protection against neurofilaments and $CD3^+$ respectively.

Effect of Treatment on NLRP3 Inflammasome.

All the treatment groups ameliorated diabetes-induced NLRP3 inflammasome activation by reducing NLRP3 (Figure 7A) and IL-1β (Figure 7B) mRNA levels compared with the diabetic group, whereas no significant changes were observed in Tnfr (Figure 7C) and CX3CR1 (Figure 7D) mRNA expression in the sciatic nerve. Similar results were obtained for spinal cord tissues, except for CUR group which was ineffective for all markers other than IL-1β (Figure 8A–D). No significant changes in NLRP3 expression in the hind paw bulb region (Figure S7A) and the ventral nerve (Figure S7B) were observed in all the groups.

Effect of Treatment on Oxidative Stress-Related Genes.

A significant reduction in the Txnrd1 mRNA level (Figure 9A) was observed in the spinal cord of diabetic rats. All treatments except nCUR failed to produce a significant effect. The mRNA levels of Srxn1 (Figure 9B) and Mt1 (Figure 9C) in the spinal cord and Txnrd1 (Figure S8) in the sciatic nerve remain unaltered across all groups.

Biochemistry and Hematology.

There was a significant increase in glucose (Figure S9A) and potassium (Figure S9B) levels, while sodium (Figure S9C), sodium–potassium ratio (Figure S9D), and calcium levels (Figure S9E) decreased in diabetic rats. Of all the treatments, nCUR+INS and INS lowered the glucose levels (Figure S9A), while all groups normalized the potassium levels, sodium–potassium ratio, and calcium (Figure S9B,D,E), except for CUR which was ineffective on lowering the potassium levels and maintaining ideal sodium–potassium ratios (Figure S9B, D). There was a significant increase in percentage (%) of monocytes (Figure S9F), neutrophils (Figure S9G), and neutrophil to lymphocyte ratio (Figure S9H) in the diabetic group and all treatment groups were significantly impactful in normalizing the changes. These findings were further corroborated by an increase in the spleen weight (normalized with body weight)/decrease in absolute spleen weight (Figure S10A,B) and an increase in lymphocyte cellularity in the spleen of diabetic rats, which were prevented in nCUR+INS (Figure S10C).

Author Manuscript Author Manuscript Author Manuscript Author Manuscript

Effect of Treatment on the Autophagy.

Significant changes in the Becn1 mRNA level (Figure S11A) were observed in spinal cord tissues for groups receiving nCUR or nCUR+INS, while all treatments were effective against sqsmt1 (Figure S11B). However, no significant difference was observed in the mRNA expression of Rheb (Figure S11C) and Pi3kC3 (Figure S11D) in the spinal cord, and Becn1 (Figure S12A), Rheb (Figure S12B), and Pi3kC3 (Figure S12C) in the sciatic nerve or their treatment groups.

DISCUSSION

DPN is one of the most common and serious secondary complications of DM. DPN can lead to loss of sensation in limbs to varying degrees which can result in falls and varying pathologies that can ultimately lead to amputation and other invasive limb salvage procedures, including amputation. Currently, this debilitating disease is managed by only using two drugs pregabalin (Lyrica) and duloxetine (Cymbalta).[22] The current approaches to keeping a tight check on glucose levels are largely ineffective in preventing diabetic complications.[23] In addition, fluctuation in glucose can trigger multiple downstream pathways involving diverse mechanisms such as protein glycation, oxidative stress, and inflammation cannot be prevented by conventional therapies.[24] Therefore, blocking one pathway or keeping a tight control on glucose levels often falls short of addressing diabetic complications and consequently requires polypharmacy that can target multiple pathways.[25–27] In this context, there is significant interest in CUR, termed as a “poster child” for its multifaceted actions in a range of diseases.[11] However, CUR undergoes extensive metabolism, leading to poor systemic bioavailability and limiting clinical translation.[28] Our prior studies showed CUR acts on various molecular targets independent of glucose reduction in the STZ-induced diabetes model,[13,21] and nCUR (PLGA-GA_2-CUR) produces a substantial increase in oral bioavailability in healthy rodents compared with the controls in the form of unformulated CUR, PLGA-CUR or PLGA-GA-CUR.[12,15,18] However, literature suggests that pathophysiology could affect the pharmacokinetics of the pharmaceutical drugs and this is more prominent with conventional dosage forms.[29] Our prior studies have shown the bioavailability of unformulated CUR was significantly influenced compared to PLGA-CUR in a model of diet-induced metabolic syndrome;[30] however, we did not measure CUR levels in the current study as the dose of unformulated CUR was 2 times higher than nCUR and because the blood was used for biochemistry and hematological parameters. On the other hand, empty particles do not have any therapeutic value and are deemed safe based on our prior studies with similar polymers and modifications.[30,31] Herein, we have studied the effect of nCUR with or without INS and compared against CUR or untreated diabetes groups and investigated possible mechanisms of actions of the combination with INS in preventing peripheral nerve damage of the hind paw, sciatic nerve, and spinal cord of STZ induced DPN in rats.

DPN is associated with dysfunction of the peripheral nerve, resulting in impaired nerve conduction and functional ability of the hind paw. As the nerve innervation in distal lower extremities of the hind paw is responsible for sensation and response, its malfunctioning impacts the quality of life. STZ-induced hyperglycemia and advanced glycation product

Author Manuscript Author Manuscript Author Manuscript Author Manuscript

(AGE) affect the structural integrity of the hind paw skin and could be responsible for the loss of hind paw skin epidermal nerve fiber innervation and cell death.[32] In support of this, analysis of the hind paw in the diabetic group showed a reduction of footpad area of hind paw after 10 weeks of diabetic induction. There was a significant reduction in neurites as demonstrated by decreased nerve fibers (Bielschowsky stained area) and IENF and NF200 expression in the hind paw of the diabetic group. These findings are consistent with a previous report[33] suggesting a clinical correlation between decreased IENF density, DPN progression, and STZ-induced changes in the hind paw.[34] Furthermore, this also emphasizes the importance of neurotrophic support of INS in epidermal nerves.[10] There was an abnormal increase in TUNEL-positive cells in diabetic rats, suggesting cell death and the possibilities of tissue damage and degeneration.[32] Our data suggest that nCUR combined with INS did better, even though the difference was not statistically significant. CUR plagued by poor oral bioavailability did fare well with a higher dose, while INS alone requires some optimization. Because CUR acts independently of glucose, we evaluated downstream inflammatory pathways. Literature reports show a correlation between macrophages ($F4/80^+$) and T cell ($CD3^+$) infiltration and inflammation in the peripheral nerve with clinically relevant mild chronic neuroinflammation.[35] Along these lines, we observed an increase in macrophage ($F4/80^+$) and T cell infiltrations ($CD3^+$) in the hind paw and sciatic nerve of diabetic rats due to chronic inflammation. The sciatic nerve is the largest peripheral nerve, and its deterioration can cause disablement in routine hind paw activities. In addition, preliminary observations suggest a reduction in the number and size of the sebaceous glands in hind paw skin of diabetic group, probably resulting in loss of moisture leading to dry skin. These observations are in line with human diabetic neuropathy symptoms specially in feet and leg where reduced sweating observed.[36] The treatment groups nCUR and nCUR+INS appears to have preserved the sebaceous glands, though their function has to be further investigated. Nestin is a class VI intermediate filament protein used as a marker for cell proliferation in the central nervous system. Downregulation of nestin is an early biomarker of vascular disease in the type I diabetes model.[37] Again, nCUR combination with INS preserves nestin expression in the sciatic nerve.

The reduction in NF200 expression and infiltration of macrophage ($F4/80^+$) and T-cell infiltrations ($CD3^+$) in sciatic nerves of diabetic rats demonstrated the involvement of macrophages and T cell infiltration in the early phase of STZ-induced peripheral neuropathy.[38] These findings were supported by high monocyte and neutrophil counts and neutrophil–lymphocyte ratio (NLR). These observations are supportive of the clinical report suggesting that patients with higher NLR are more likely to develop peripheral neuropathy.[39,40] The increase in the weight of spleen and white pulp in spleen suggests an increase in lymphocyte cellularity, which may indicate diabetic-associated immune cell activation.[35] Again, nCUR with or without INS regulates the immune system activation due to its anti-inflammatory property and is in accordance with earlier reports.[41,42]

There is a significant increase in the expression of NLRP3, suggesting its activation leads to maturation and further release of IL-1β in the sciatic nerve of diabetic rats.[43] Furthermore, blood biochemistry demonstrates an increase in K^+ and a decrease in Ca^{2+} in the plasma. Change in the K^+ concentration is considered a crucial event during NLRP3 inflammasome activation because K^+ efflux alone can activate NLRP3 and potentiates IL-1β

Author Manuscript Author Manuscript Author Manuscript Author Manuscript

maturation.[44,45] The combination treatment was effective if not better than nCUR alone. The trends indicate a reduction in the Tnfr and CX3CR1 expression, although the effects were not significant in the sciatic nerve probably due to interindividual variability.

There is an increase in the levels of NLRP3, IL-1β, Tnfr, and CX3CR1 in the spinal cord of diabetic rats. Furthermore, the NLRP3 pathway is closely associated with mitochondria oxidative stress that correlates well with a reduction in Txnrd1 expression. These observations are in accordance with previous reports[46,47] demonstrating the role of Txnrd1 in DPN, and the combination treatment seems to work well, if not better than nCUR alone.

CONCLUSION

In conclusion, we combined nCUR with subcutaneous long-acting INS with the intent of targeting multiple progressive pathways in DM. Our data suggest that nCUR with or without INS alleviates DPN-associated changes by modulating the immunoinflammatory pathway. The combination and nCUR alone reduced macrophage infiltration, NLRP3 activation and IL-1β maturation. Overall, this is a first-of-its-kind preclinical evaluation of nCUR and its combination with INS in the DPN model. Therefore, it is important to further test its clinical efficacy by adjusting regimens or even using an oral INS format, instead of subcutaneous INS.

Supplementary Material

Refer to Web version on PubMed Central for supplementary material.

ACKNOWLEDGMENTS

The authors thank Dr. Dianxiong Zou for imaging and analysis of the inked impression of the hind paw pad area.

Funding

This work is supported in parts by National Institutes of Health Grants (Nos: R01EY028169, R01DK125372).

ABBREVIATIONS

AUC	area under curve
C_{max}	maximum concentration/peak
CUR	curcumin
CX3CL1	chemokine (C-X3-C motif) receptor 1
IENF	intraepidermal nerve fiber-IL-1β-interleukin-1β
GA	gambogic acid
NLRP3	Nod-like receptor family pyrin domain containing 3
mRNA	mRNA

Author Manuscript Author Manuscript Author Manuscript Author Manuscript

NF200	neurofilament 200
nCUR	curcumin-laden double-headed nanoparticles
PLGA	GA_2-terminal carboxyl group of PLGA conjugated to two molecules of GA
Txnrd1	thioredoxin reductase 1
Tnfr	tumor necrosis factor receptor

REFERENCES

(1). Sun H; Saeedi P; Karuranga S; Pinkepank M; Ogurtsova K; Duncan BB; Stein C; Basit A; Chan JCN; Mbanya JC; et al. IDF Diabetes Atlas: Global, regional and country-level diabetes prevalence estimates for 2021 and projections for 2045. Diabetes Res. Clin Pract 2022, 183, 109119. [PubMed: 34879977]

(2). Hicks CW; Selvin E Epidemiology of Peripheral Neuropathy and Lower Extremity Disease in Diabetes. Curr. Diab Rep 2019, 19 (10), 86. [PubMed: 31456118]

(3). Pop-Busui R; Boulton AJ; Feldman EL; Bril V; Freeman R; Malik RA; Sosenko JM; Ziegler D Diabetic Neuropathy: A Position Statement by the American Diabetes Association. Diabetes Care 2017, 40 (1), 136–154. [PubMed: 27999003]

(4). Feldman EL; Callaghan BC; Pop-Busui R; Zochodne DW; Wright DE; Bennett DL; Bril V; Russell JW; Viswanathan V Diabetic neuropathy. Nat. Rev. Dis Primers 2019, 5 (1), 41. [PubMed: 31197153]

(5). Sandireddy R; Yerra VG; Areti A; Komirishetty P; Kumar A Neuroinflammation and oxidative stress in diabetic neuropathy: futuristic strategies based on these targets. Int. J. Endocrinol 2014, 2014, 674987. [PubMed: 24883061]

(6). Vinik AI; Mehrabyan A Diabetic neuropathies. Med. Clin North Am 2004, 88 (4), 947–999. [PubMed: 15308387]

(7). Yang H; Sloan G; Ye Y; Wang S; Duan B; Tesfaye S; Gao L New Perspective in Diabetic Neuropathy: From the Periphery to the Brain, a Call for Early Detection, and Precision Medicine. Front Endocrinol (Lausanne) 2020, 10, 929. [PubMed: 32010062]

(8). Callaghan BC; Little AA; Feldman EL; Hughes RAEnhanced glucose control for preventing and treating diabetic neuropathy. Cochrane Database Syst. Rev2012, (6) DOI: 10.1002/14651858.CD007543.pub2.

(9). Tesfaye S; Wilhelm S; Lledo A; Schacht A; Tolle T; Bouhassira D; Cruccu G; Skljarevski V; Freynhagen R Duloxetine and pregabalin: high-dose monotherapy or their combination? The “COMBO-DN study”-a multinational, randomized, double-blind, parallel-group study in patients with diabetic peripheral neuropathic pain. Pain 2013, 154 (12), 2616–2625. [PubMed: 23732189]

(10). Toth C; Brussee V; Zochodne DW Remote neurotrophic support of epidermal nerve fibres in experimental diabetes. Diabetologia 2006, 49 (5), 1081–1088. [PubMed: 16528572]

(11). Corson TW; Crews CM Molecular understanding and modern application of traditional medicines: triumphs and trials. Cell 2007, 130 (5), 769–774. [PubMed: 17803898]

(12). Kaur G; Arora M; Ganugula R; Kumar MNVR Double-headed nanosystems for oral drug delivery. Chem. Commun. (Camb) 2019, 55 (33), 4761–4764. [PubMed: 30869656]

(13). Grama CN; Suryanarayana P; Patil MA; Raghu G; Balakrishna N; Kumar MNVR; Reddy GB Efficacy of biodegradable curcumin nanoparticles in delaying cataract in diabetic rat model. PLoS One 2013, 8 (10), No. e78217. [PubMed: 24155984]

(14). Joshi RP; Negi G; Kumar A; Pawar YB; Munjal B; Bansal AK; Sharma SS SNEDDS curcumin formulation leads to enhanced protection from pain and functional deficits associated with diabetic neuropathy: an insight into its mechanism for neuroprotection. Nanomedicine 2013, 9 (6), 776–785. [PubMed: 23347896]

Author Manuscript Author Manuscript Author Manuscript Author Manuscript

(15). Ganugula R; Arora M; Lepiz MA; Niu Y; Mallick BK; Pflugfelder SC; Scott EM; Kumar MNVR Systemic anti-inflammatory therapy aided by double-headed nanoparticles in a canine model of acute intraocular inflammation. Sci. Adv 2020, 6 (35), No. eabb7878. [PubMed: 32923645]

(16). Ucisik MH; Kupcu S; Schuster B; Sleytr UB Characterization of CurcuEmulsomes: nanoformulation for enhanced solubility and delivery of curcumin. J. Nanobiotechnology 2013, 11, 37. [PubMed: 24314310]

(17). Bala I; Hariharan S; Kumar MN PLGA nanoparticles in drug delivery: the state of the art. Crit Rev. Ther Drug Carrier Syst 2004, 21 (5), 387–422. [PubMed: 15719481]

(18). Shaikh J; Ankola DD; Beniwal V; Singh D; Kumar MNVR Nanoparticle encapsulation improves oral bioavailability of curcumin by at least 9-fold when compared to curcumin administered with piperine as absorption enhancer. Eur. J. Pharm. Sci 2009, 37 (3–4), 223–230. [PubMed: 19491009]

(19). Grama CN; Venkatpurwar VP; Lamprou DA; Kumar MNVR Towards scale-up and regulatory shelf-stability testing of curcumin encapsulated polyester nanoparticles. Drug Deliv Transl Res. 2013, 3 (3), 286–293. [PubMed: 25788136]

(20). Yerra VG; Kumar A Adenosine Monophosphate-Activated Protein Kinase Abates Hyperglycaemia-Induced Neuronal Injury in Experimental Models of Diabetic Neuropathy: Effects on Mitochondrial Biogenesis, Autophagy and Neuroinflammation. Mol. Neurobiol 2017, 54 (3), 2301–2312. [PubMed: 26957299]

(21). Ganugula R; Arora M; Jaisamut P; Wiwattanapatapee R; Jorgensen HG; Venkatpurwar VP; Zhou B; Rodrigues Hoffmann A; Basu R; Guo S; et al. Nano-curcumin safely prevents streptozotocin-induced inflammation and apoptosis in pancreatic beta cells for effective management of Type 1 diabetes mellitus. Br. J. Pharmacol 2017, 174 (13), 2074–2084. [PubMed: 28409821]

(22). Snyder MJ; Gibbs LM; Lindsay TJ Treating Painful Diabetic Peripheral Neuropathy: An Update. Am. Fam Physician 2016, 94 (3), 227–234. [PubMed: 27479625]

(23). Kobayati A; Haidar A; Tsoukas MA GLP-1 Receptor Agonists as Adjunctive Treatment for Type 1 Diabetes: Renewed Opportunities through Tailored Approaches? Diabetes Obes Metab 2022, 24, 769. [PubMed: 34989070]

(24). Zhang ZY; Miao LF; Qian LL; Wang N; Qi MM; Zhang YM; Dang SP; Wu Y; Wang RX Molecular Mechanisms of Glucose Fluctuations on Diabetic Complications. Front Endocrinol (Lausanne) 2019, 10, 640. [PubMed: 31620092]

(25). Manigrasso MB; Rabbani P; Egana-Gorrono L; Quadri N; Frye L; Zhou B; Reverdatto S; Ramirez LS; Dansereau S; Pan J; et al. Small-molecule antagonism of the interaction of the RAGE cytoplasmic domain with DIAPH1 reduces diabetic complications in mice. Sci. Transl Med 2021, 13 (621), No. eabf7084. [PubMed: 34818060]

(26). Artasensi A; Pedretti A; Vistoli G; Fumagalli L Type 2 Diabetes Mellitus: A Review of Multi-Target Drugs. Molecules 2020, 25 (8), 1987. [PubMed: 32340373]

(27). Daugherty DJ; Marquez A; Calcutt NA; Schubert D A novel curcumin derivative for the treatment of diabetic neuropathy. Neuropharmacology 2018, 129, 26–35. [PubMed: 29122628]

(28). Esatbeyoglu T; Huebbe P; Ernst IM; Chin D; Wagner AE; Rimbach G Curcumin-from molecule to biological function. Angew. Chem., Int. Ed. Engl 2012, 51 (22), 5308–5332. [PubMed: 22566109]

(29). Ye LX; Huang HH; Zhang SH; Lu JS; Cao DX; Wu DD; Chi PW; Hong LH; Wu MX; Xu Y; et al. Streptozotocin-Induced Hyperglycemia Affects the Pharmacokinetics of Koumine and its Anti-Allodynic Action in a Rat Model of Diabetic Neuropathic Pain. Front Pharmacol 2021, 12, 640318. [PubMed: 34054521]

(30). du Preez R; Pahl J; Arora M; Kumar MNVR; Brown L; Panchal SK Low-Dose Curcumin Nanoparticles Normalise Blood Pressure in Male Wistar Rats with Diet-Induced Metabolic Syndrome. Nutrients 2019, 11 (7), 1542. [PubMed: 31288419]

(31). Arora M; Ganugula R; Kumar N; Kaur G; Pellois J-P; Garg P; Kumar MNVR Next-Generation Noncompetitive Nanosystems Based on Gambogic Acid: In silico Identification of Transferrin Receptor Binding Sites, Regulatory Shelf Stability, and Their Preliminary Safety in Healthy Rodents. ACS Appl. Bio Mater 2019, 2 (8), 3540–3550.

Author Manuscript Author Manuscript Author Manuscript Author Manuscript

(32). Noh SU; Lee WY; Kim WS; Lee YT; Yoon KJExpression of macrophage migration inhibitory factor in footpad skin lesions with diabetic neuropathy. Mol. Pain 2018, 14, 1744806918775482 [PubMed: 29690804]

(33). Timar B; Popescu S; Timar R; Baderca F; Duica B; Vlad M; Levai C; Balinisteanu B; Simu M The usefulness of quantifying intraepidermal nerve fibers density in the diagnostic of diabetic peripheral neuropathy: a cross-sectional study. Diabetol Metab Syndr 2016, 8, 31. [PubMed: 27069510]

(34). Ozaki K; Terayama Y; Matsuura T Extended Duration of Hyperglycemia Result in Human-Like Corneal Nerve Lesions in Mice With Alloxan- and Streptozotocin-Induced Type 1 Diabetes. Invest Ophthalmol Vis Sci. 2018, 59 (15), 5868–5875. [PubMed: 30550618]

(35). Baum P; Kosacka J; Estrela-Lopis I; Woidt K; Serke H; Paeschke S; Stockinger M; Kloting N; Bluher M; Dorn M; et al. The role of nerve inflammation and exogenous iron load in experimental peripheral diabetic neuropathy (PDN). Metabolism 2016, 65 (4), 391–405. [PubMed: 26975531]

(36). Cardone C; Dyck PJ A neuropathic deficit, decreased sweating, is prevented and ameliorated by euglycemia in streptozocin diabetes in rats. J. Clin Invest 1990, 86 (1), 248–253. [PubMed: 2195061]

(37). Tardif K; Hertig V; Dumais C; Villeneuve L; Perrault L; Tanguay JF; Calderone A Nestin downregulation in rat vascular smooth muscle cells represents an early marker of vascular disease in experimental type I diabetes. Cardiovasc Diabetol 2014, 13, 119. [PubMed: 25139503]

(38). Conti G; Scarpini E; Baron P; Livraghi S; Tiriticco M; Bianchi R; Vedeler C; Scarlato G Macrophage infiltration and death in the nerve during the early phases of experimental diabetic neuropathy: a process concomitant with endoneurial induction of IL-1beta and p75NTR. J. Neurol Sci 2002, 195 (1), 35–40. [PubMed: 11867071]

(39). Xu T; Weng Z; Pei C; Yu S; Chen Y; Guo W; Wang X; Luo P; Sun J The relationship between neutrophil-to-lymphocyte ratio and diabetic peripheral neuropathy in Type 2 diabetes mellitus. Medicine (Baltimore) 2017, 96 (45), No. e8289. [PubMed: 29137012]

(40). Liu S; Zheng H; Zhu X; Mao F; Zhang S; Shi H; Li Y; Lu B Neutrophil-to-lymphocyte ratio is associated with diabetic peripheral neuropathy in type 2 diabetes patients. Diabetes Res. Clin Pract 2017, 130, 90–97. [PubMed: 28582723]

(41). Sun JJ; Tang L; Zhao XP; Xu JM; Xiao Y; Li H Infiltration of Blood-Derived Macrophages Contributes to the Development of Diabetic Neuropathy. J. Immunol. Res 2019, 2019, 7597382. [PubMed: 31534976]

(42). Young NA; Bruss MS; Gardner M; Willis WL; Mo X; Valiente GR; Cao Y; Liu Z; Jarjour WN; Wu LC Oral administration of nano-emulsion curcumin in mice suppresses inflammatory-induced NFkappaB signaling and macrophage migration. PLoS One 2014, 9 (11), No. e111559. [PubMed: 25369140]

(43). Yin Y; Chen F; Wang W; Wang H; Zhang X Resolvin D1 inhibits inflammatory response in STZ-induced diabetic retinopathy rats: Possible involvement of NLRP3 inflammasome and NF-kappaB signaling pathway. Mol. Vis 2017, 23, 242–250. [PubMed: 28465656]

(44). Walev I; Klein J; Husmann M; Valeva A; Strauch S; Wirtz H; Weichel O; Bhakdi S Potassium regulates IL-1 beta processing via calcium-independent phospholipase A2. J. Immunol 2000, 164 (10), 5120–5124. [PubMed: 10799869]

(45). Munoz-Planillo R; Kuffa P; Martinez-Colon G; Smith BL; Rajendiran TM; Nunez G K(+) efflux is the common trigger of NLRP3 inflammasome activation by bacterial toxins and particulate matter. Immunity 2013, 38 (6), 1142–1153. [PubMed: 23809161]

(46). Ren X; Li C, Liu J; Zhang C, Fu Y; Wang N; Ma H; Lu H; Kong H; Kong L Thioredoxin plays a key role in retinal neuropathy prior to endothelial damage in diabetic mice. Oncotarget 2017, 8 (37), 61350–61364. [PubMed: 28977868]

(47). Miao J; Zhou X; Ji T; Chen G NF-kappaB p65-dependent transcriptional regulation of histone deacetylase 2 contributes to the chronic constriction injury-induced neuropathic pain via the micro-RNA-183/TXNIP/NLRP3 axis. J. Neuroinflammation 2020, 17 (1), 225. [PubMed: 32723328]

Author Manuscript
Author Manuscript
Author Manuscript
Author Manuscript

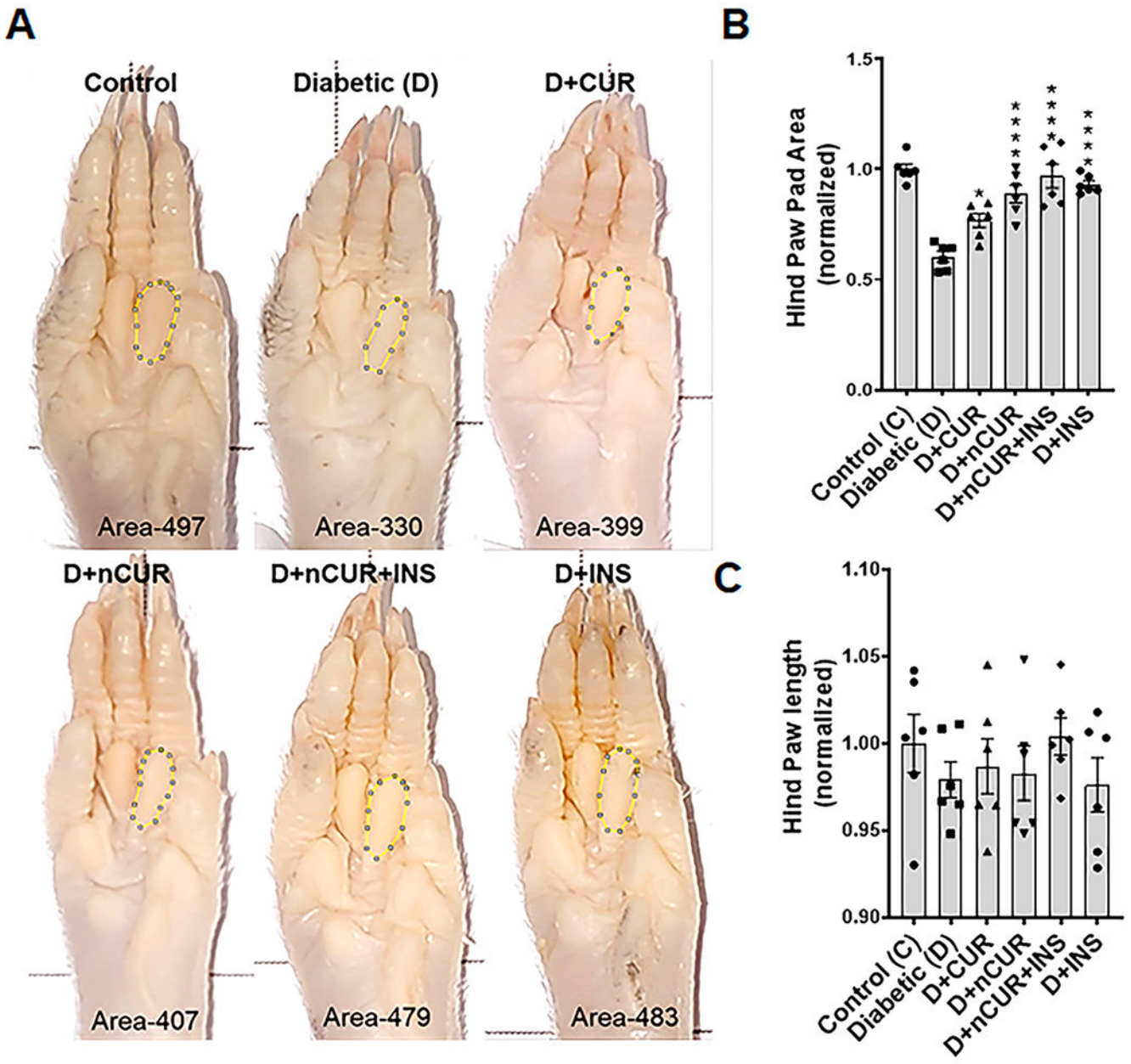

Figure 1.

(A) Representative images of the right hind paw pad showing manually marked second bulb area used for quantification. (B) Summary of the normalized area of the hind paw (at least n = 6 images were used for quantification). (C) Summary of the normalized hind paw length of all experimental groups. Statistical analysis was carried out using one-way ANOVA and Tukey posthoc test. Significance values were compared against the diabetic group: *, $P < 0.05$; ****, $P < 0.0001$.

Author Manuscript Author Manuscript Author Manuscript Author Manuscript

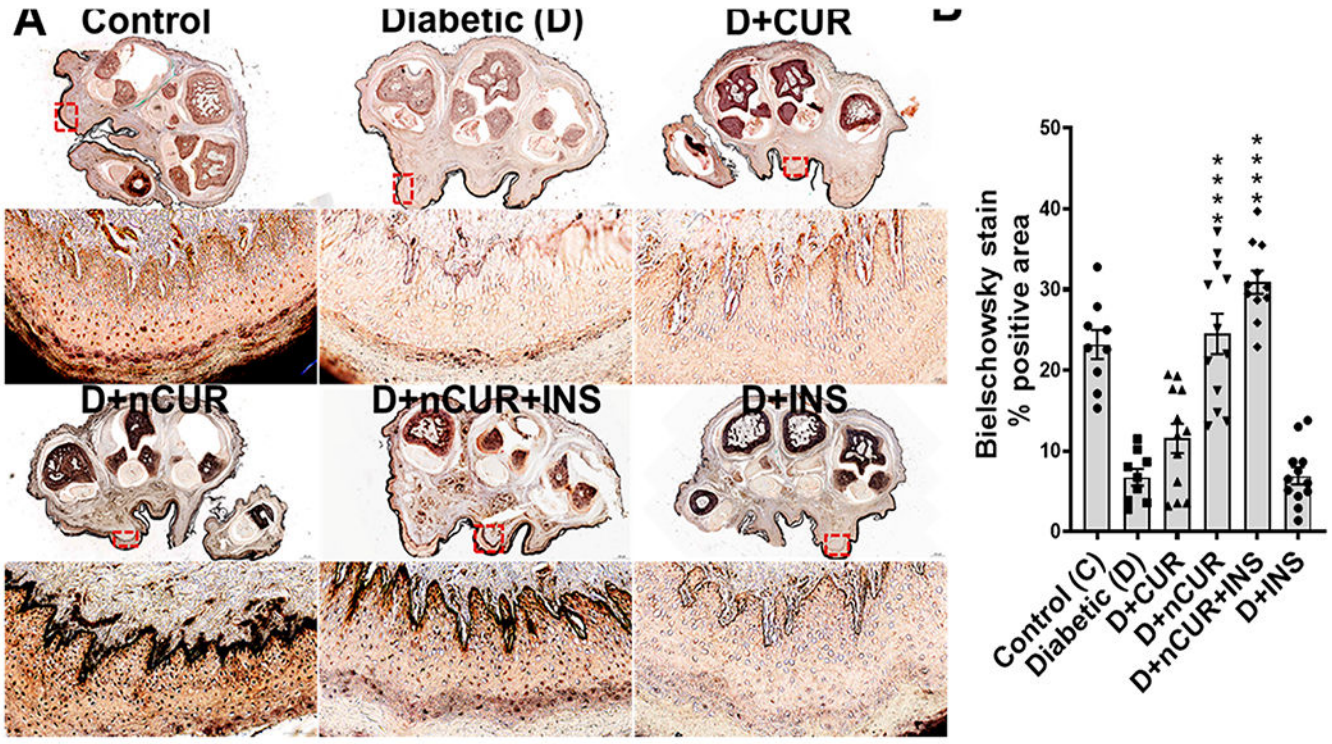

Figure 2.

(A) Representative images (upper at a scale of 500 μm) with the Bielschowsky staining of a transverse section of the whole right hind paw and the globulus hind paw skin magnified images (scale bar, 20 μm) of selected red box areas further analyzed for quantification (all images in the higher magnification-oriented uniformly). (B) Quantitative (n = 8 images) analysis of the Bielschowsky staining. Statistical analysis was carried out using one-way ANOVA and Tukey post hoc test. Significant values were compared with the diabetic group: ****, $P < 0.001$.

Author Manuscript Author Manuscript Author Manuscript Author Manuscript

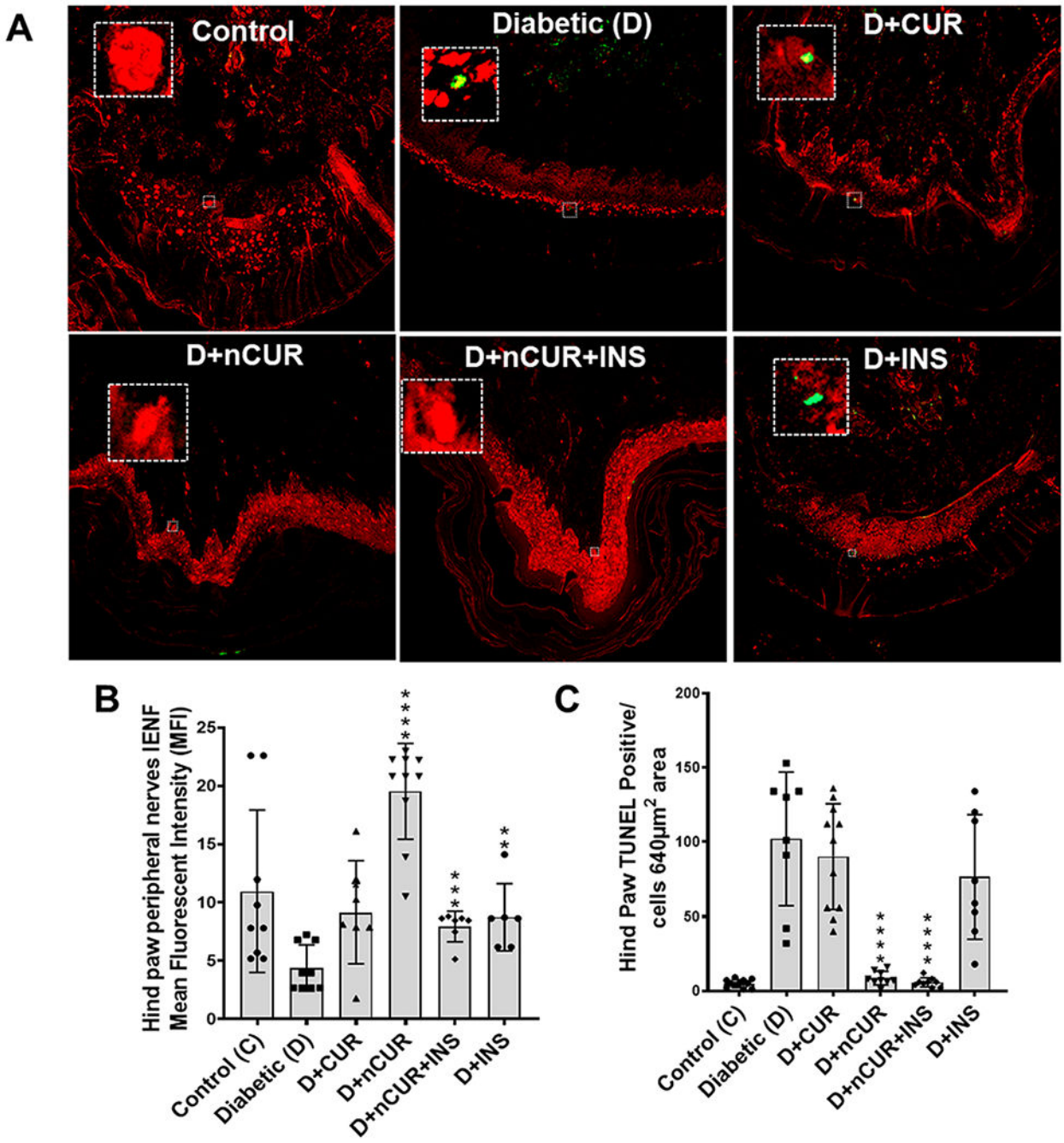

Figure 3.

Representative images of IENF and TUNEL stains in peripheral nerve of the right hind paw of all studied groups. (A) Cross section of the peripheral nerve of the hind paw stained with an IENF antibody (red) at 20× magnification. (B) Quantitative representation of IENF expression. (C) TUNEL staining (green) of the selected area (white box from panel A images) in the peripheral nerve of the hind paw used for quantification (n = 8 images) representing TUNEL-positive cells. Statistical analysis was carried out using one-way ANOVA and Tukey posthoc test for TUNEL and Student's t test for IENF staining.

Author Manuscript Author Manuscript Author Manuscript Author Manuscript

Significant values were compared with the diabetic group: *, $P < 0.05$; **, $P < 0.01$; ***, $P < 0.001$; ****, $P < 0.0001$.

Author Manuscript Author Manuscript Author Manuscript Author Manuscript

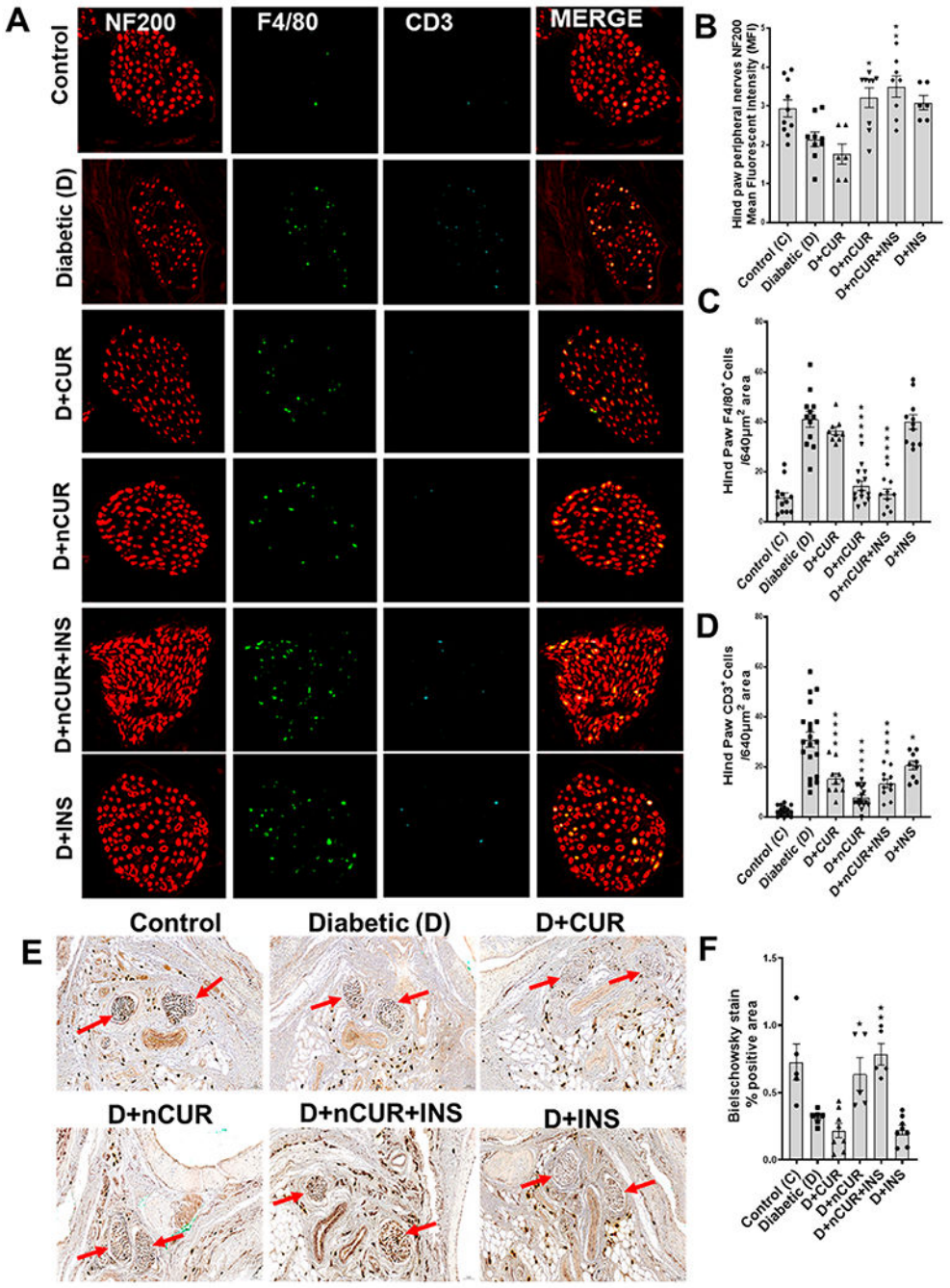

Figure 4.

Representative images of peripheral nerve fibers of the right hind paw stained for NF200 expression and F4/80- and CD3-positive cells. (A) Cross section of peripheral nerve fibers of hind paw showing NF200 expression (red) and F4/80- (green), and CD3-positive (turquoise) cells (digitally magnified from the original images presented in Figure S4A). The bar charts represent the outcomes of quantitative analysis for (n = 8 images) (B) NF200 expression and (C) F4/80- and (D) CD3-positive cells. (E) Bielschowsky staining of a cross section of the right hind paw and the peripheral nerve (indicated by the red arrow) of globulus hind paw

Author Manuscript Author Manuscript Author Manuscript Author Manuscript

magnified images (at 20× magnification) ($n = 5$ images used for quantification). Statistical analysis was carried out using one-way ANOVA and Tukey's posthoc test and Student's t test for Bielschowsky staining for peripheral nerves. Significant values were compared with the diabetic group: *, $P < 0.05$; **, $P < 0.01$; and ****, $P < 0.0001$.

Author Manuscript Author Manuscript Author Manuscript Author Manuscript

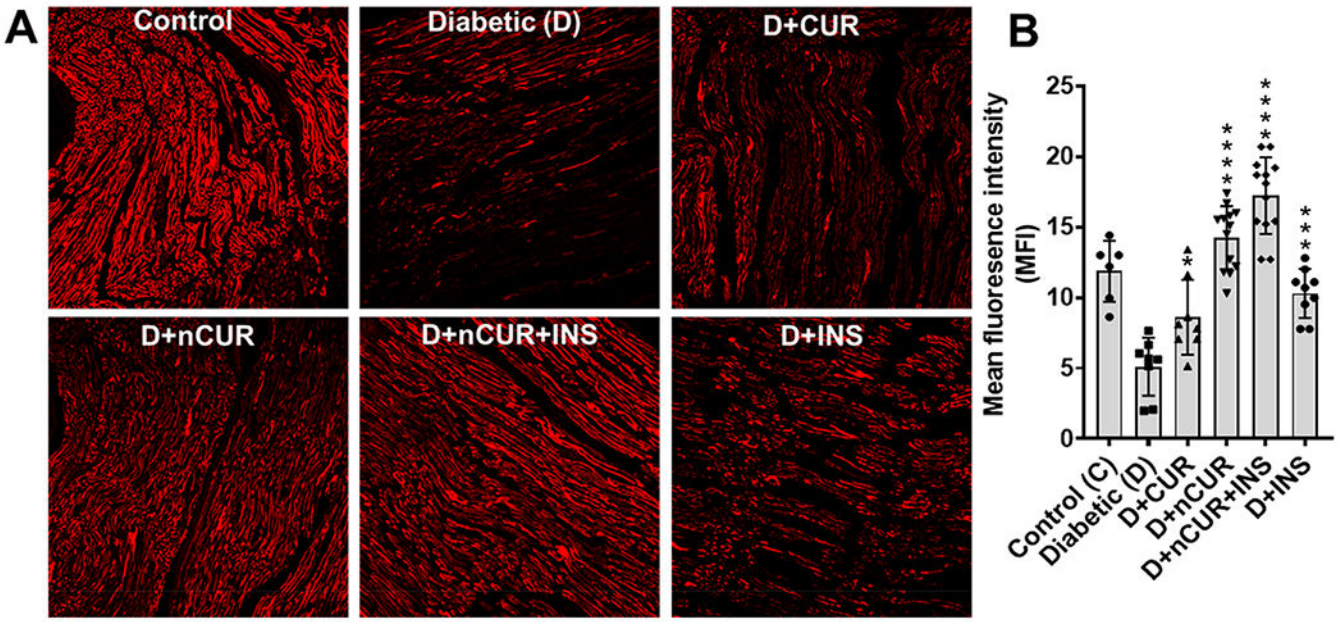

Figure 5.

Nestin expression in the sciatic nerve. (A) Representative images (20× magnification) of the vertical section with nestin (red) are presented. (B) Quantitative ($n = 8$ images) analysis showing nestin expression. Statistical analysis was carried out using one-way ANOVA and Tukey's posthoc test. Significant values were compared with the diabetic group: *. $P < 0.05$; ***, $P < 0.001$; and ****, $P < 0.0001$.

Author Manuscript Author Manuscript Author Manuscript Author Manuscript

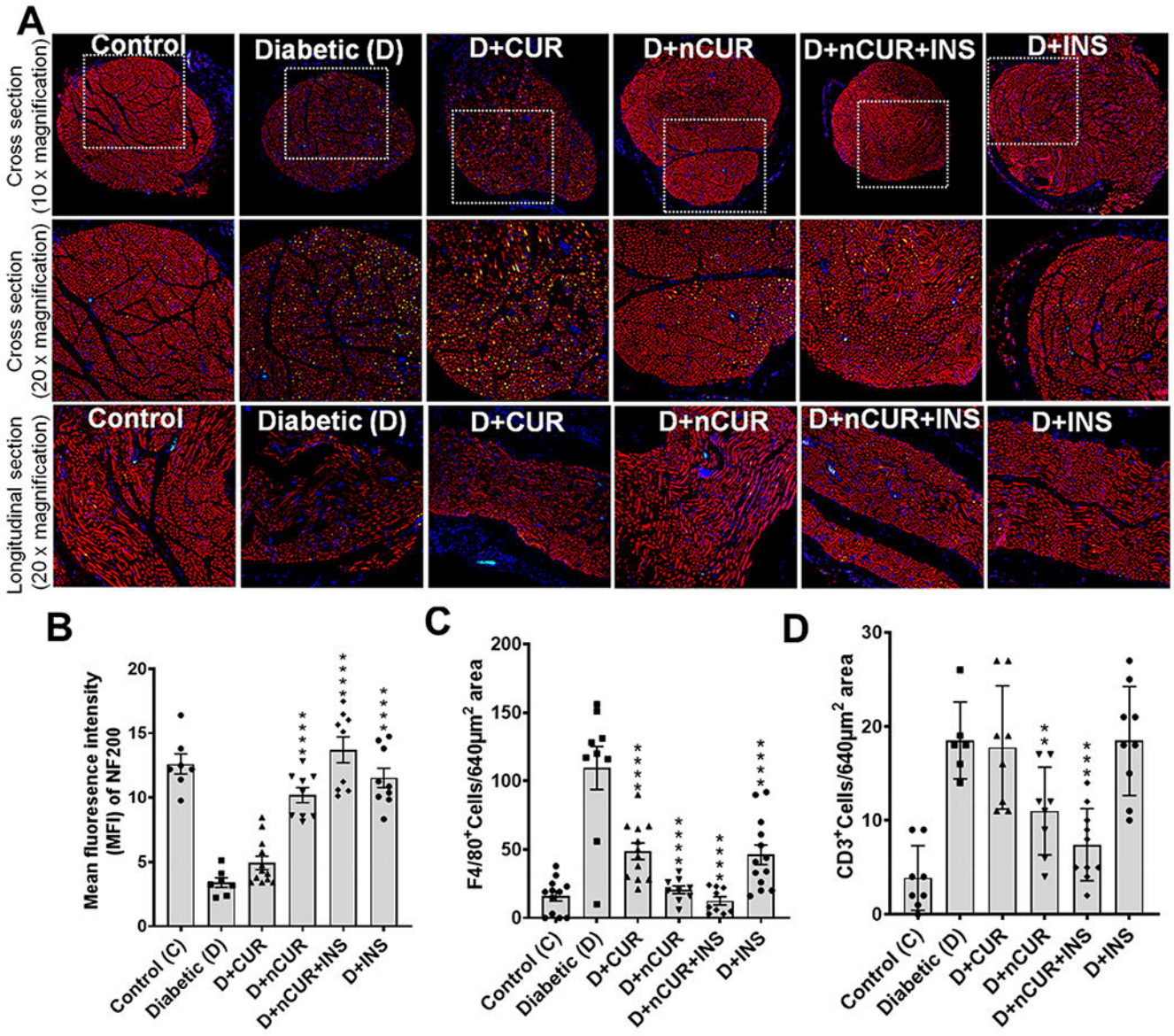

Figure 6.

Representative images of the sciatic nerve stained for NF200, F4/80-positive, and CD3-positive cells. (A) Cross section of the sciatic nerve at 10× magnification, magnified images of the selected area (white box) at 20× magnification, and longitudinal sections at 20× magnification showing NF200 expression (red) and F4/80- (green) and CD3-positive (turquoise) cells staining used for quantification ($n = 8$ images). (B) NF 200-, (C) F4/80-, and (D) CD3-positive cells. Statistical analysis was carried out using one-way ANOVA and Tukey posthoc test except that student t test was used for CD3-positive cells. Significant values were compared with the diabetic group: **, $P < 0.01$; ***, $P < 0.001$; and ****, $P < 0.0001$. Individual and merged images of sciatic nerve stained for NF200 expression and F4/80- and CD3-positive cells were presented in Figure S6.

Author Manuscript Author Manuscript Author Manuscript Author Manuscript

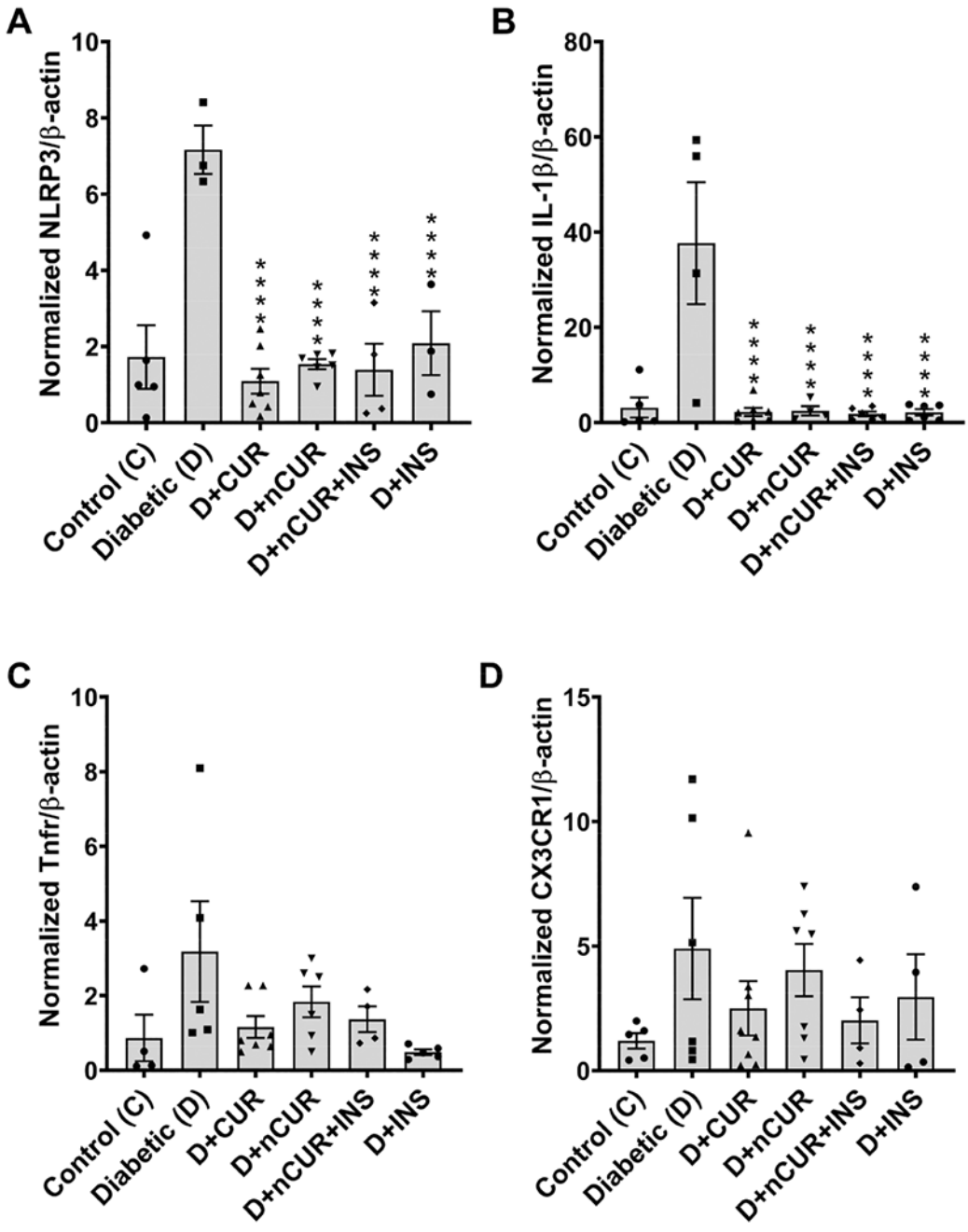

Figure 7.

NLRP3 inflammasome in the sciatic nerve. Real-time PCR data show the mRNA level of (A) NLRP3, (B) IL-1β, (C) Tnfr, and (D) CX3CR1. Statistical analysis was carried out using one-way ANOVA and Tukey's posthoc test. Significant values were compared with the diabetic group: ****, $P < 0.0001$.

Author Manuscript Author Manuscript Author Manuscript Author Manuscript

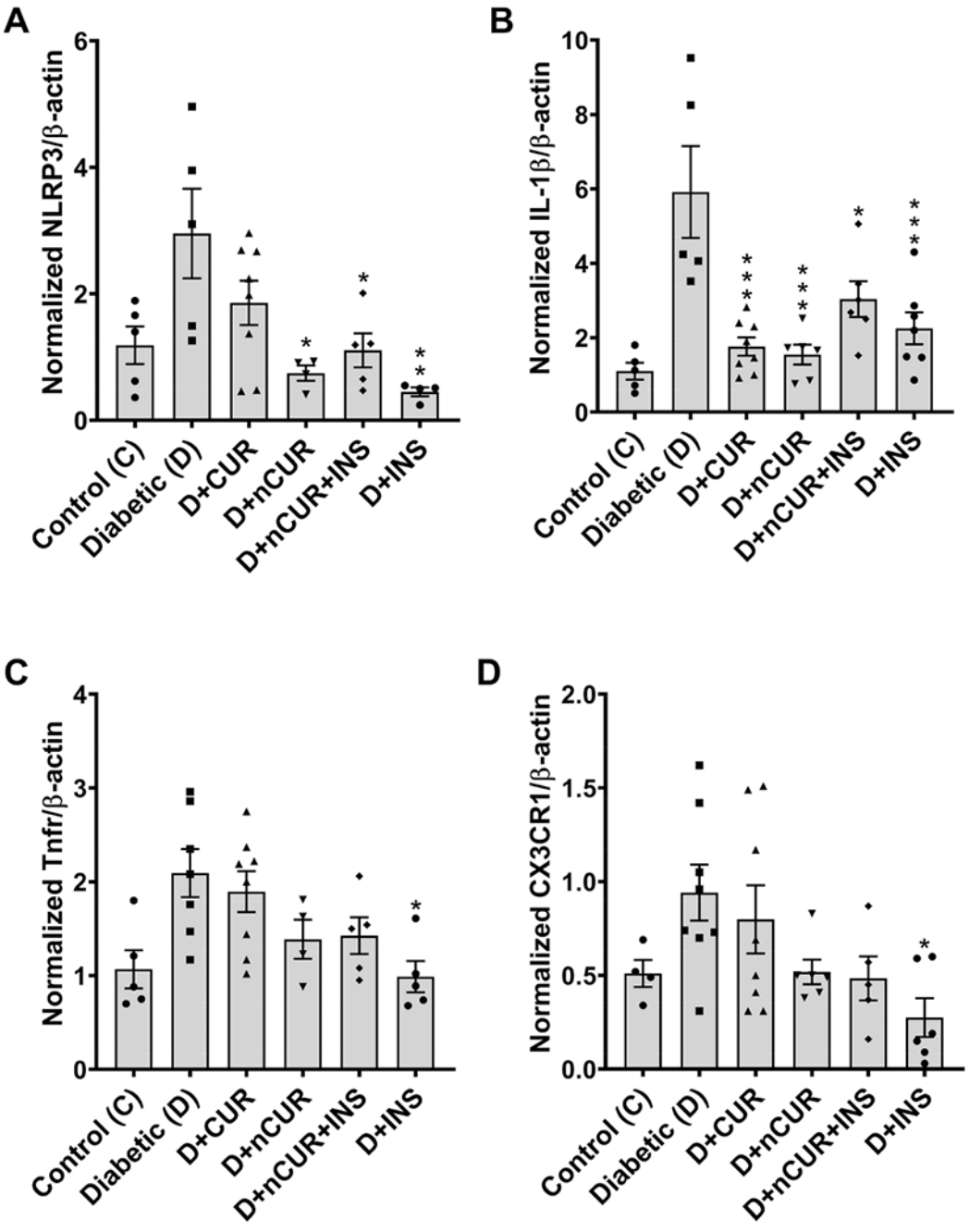

Figure 8.

NLRP3 inflammasome in the spinal cord. Real-time PCR data show the mRNA levels of (A) NLRP3, (B) IL-1*β*, (C) Tnfr, and (D) CX3CR1. Statistical analysis was carried out using one-way ANOVA and Tukey's posthoc. Significant values were compared with the diabetic group: *, $P < 0.05$; **, $P < 0.01$; and ***, $P < 0.001$.

Author Manuscript Author Manuscript Author Manuscript Author Manuscript

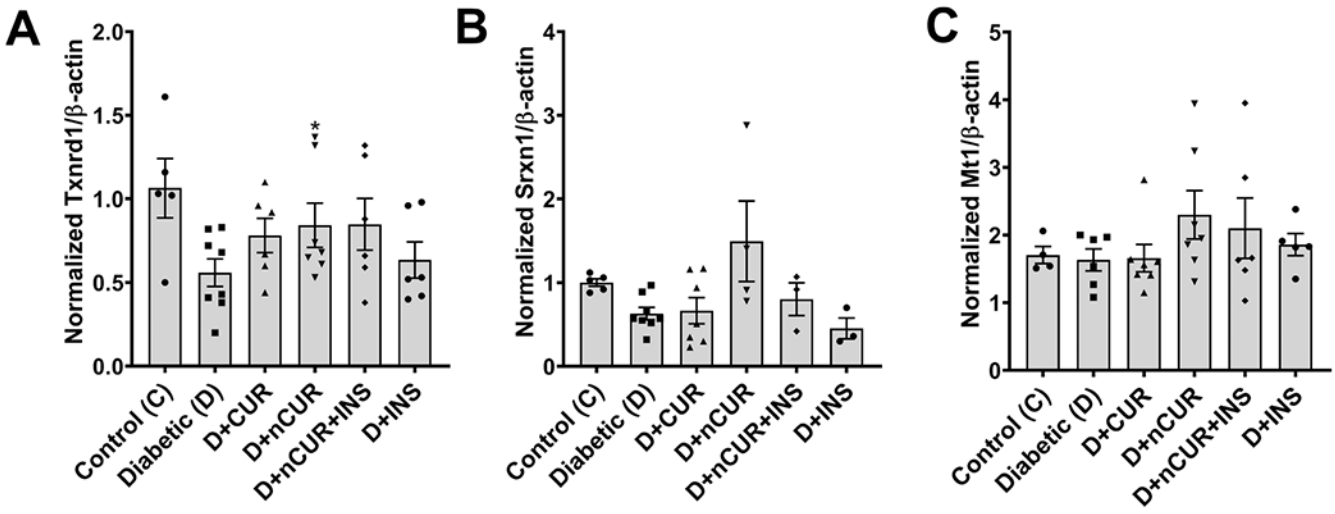

Figure 9.

Expression of oxidative stress-related genes in the spinal cord. Real time PCR data show the mRNA level of (A) Txnrd1, (B) Srxn1, and (C) Mt1. Statistical analysis was carried out using the student *t* test. Significant values were compared with the diabetic group: *, $P < 0.05$.

Author Manuscript Author Manuscript Author Manuscript Author Manuscript

Table 1.

List of Primers Used in qPCR

gene name[a]	primer sequence forward	primer sequence reverse
NLRP3	5′GGCCAGATGGAGAAGGCAG3′	5′CAGAGGTCTCGCCTGTTGAT3′
IL1β	5′CCTGCAGCTGGAGAGTGTG3′	5′GCTGATGTACCAGTTGGGGA3′
TNFRSF1A	5′AACACCGTGTGTAACTGCCA3′	5′GTCCTGGGGGTTTGTGACAT3′
CX3CR1	5′GAGTATGACGATTCTGCTGAG3′	5′CAGACCGAACGTGAAGACGAG3′
TXNRD1	5′CCCACTTGCCCCAACTGTT3′	5′GGGAGTGTCTTGGAGGGAC3′
SRXN1	5′GCCAAGCTCGTGAGGTCTAC3′	5′TGGGGTATCAGGAGGTTGCT3′
MT1	5′CTGCTGCCCTCAGGTGTAAA3′	5′ATGCTCGGTAGAAAACGGGG3′
BECN1	5′CAACCCCATGCTGTCCTTTC3′	5′GTGTGCCACAAGCATCTCATC3′
RHEB-1	5′CGATAGTCTGAGCCGGAGGA3′	5′ACAGACCGATAGCCCAGGAT3′
PIK3C3	5′TCATTACACCAACCCCACCG3′	5′TGGTAGGCTCCAAACCGTTC3′
SQSTM1	5′GATAGCCTTGGAGTCGGTGG3′	5′CCTGTGGATGGGTCCACTTC3′
β-actin	5′CTCTGTGTGGATTGGTGGCT3′	5′AGCTCAGTAACAGTCCGCCT3′

[a]NLRP3, Nod-like receptor family pyrin domain containing 3; IL-1β interleukin-1β; Tnfr, tumor necrosis factor receptor superfamily member 1A; CX3CL1, chemokine (C-X3-C motif) receptor 1; Txnrd1, thioredoxin reductase 1; Mt1, metallothionein 1; Srxn1, sulfiredoxin 1 homologue; Becn1, beclin 1; Rheb-1, Ras homologue enriched in the brain; Pik3c3, Class III phosphatidylinositol 3-kinase; Sqstm1, sequestosome 1; β-actin.

Mol Pharm. Author manuscript; available in PMC 2023 December 05.